

**LONGITUDINAL SAMPLING REVEALS LOCAL IMPACTS
TO STREAM BIOGEOCHEMISTRY IN A TROPICAL WATERSHED**

A THESIS SUBMITTED TO THE GRADUATE DIVISION OF
THE UNIVERSITY OF HAWAI'I AT MĀNOA IN PARTIAL FULFILLMENT
OF THE REQUIREMENTS FOR THE DEGREE OF

MASTER OF SCIENCE

IN

OCEANOGRAPHY

August 2021

By

Sean H. Mahaffey

Thesis Committee:

Brian Glazer, Chairperson

Margaret McManus

Craig Nelson

ACKNOWLEDGEMENTS

The journey culminating in this thesis has been a meandering and at times difficult one. Numerous expected and unexpected challenges, including a global pandemic, tested my limits and nearly pushed me past my breaking point more than once. Although graduate school is isolating at times, the community surrounding me was always there for support and encouragement and it was through this community that I was able to persevere and succeed. I sincerely want to thank my committee members, Professors Brian Glazer, Margaret McManus, and Craig Nelson, for their time, support, guidance, and mentorship; the oceanography department faculty for teaching in and out of the classroom as well as always being available as a resource; the oceanography staff for making this a warm and welcoming environment; the graduate students and specifically my cohort who have shared this time with me and have made it their mission to not only improve our department but also the world around us. I want to specifically acknowledge and thank Jessica Bullington for her assistance in getting me up and running on this project as well as wrangling data; and Aka Beebe for doing the leg work collecting samples and making measurements; this work was not possible without both of you. My friends have always been a pillar in my life, thank you for the never-ending support and friendship. Lastly, this all began with my family, to whom I am forever grateful for. Thank you to my parents for instilling in me a love for the environment and the great outdoors, and to my siblings for all our adventures.

It's a magical world, Hobbes, ol' buddy... Let's go exploring!

—Bill Watterson, CALVIN AND HOBBS

FUNDING

This work was supported by the Strategic Monitoring and Resilience Training in the Ala Wai Watershed (SMART Ala Wai) project which was funded by the Vice Chancellor for Research at the University of Hawai‘i at Mānoa through the Strategic Investment Initiative.

Additional funding was provided by the John and Anne Flanigan Oceanography Support Fund.

This material is based upon work supported by the National Science Foundation Graduate Research Fellowship Program under Grant No. 1842402. Any opinions, findings, and conclusions or recommendations expressed in this material are those of the author and do not necessarily reflect the views of the National Science Foundation.

ABSTRACT

The Ala Wai Watershed on the island of O‘ahu, Hawai‘i is 42.4 square kilometers in area, drained by three stream systems, Makiki, Mānoa, and Pālolo discharging into the Ala Wai Canal, is densely urbanized in the mid and lower reaches, and has forested areas along the upper valleys and valley ridges. The Ala Wai Canal was constructed in the early 20th century to drain the Waikīkī wetland and the three streams were subsequently altered to direct flow and prevent flooding. Measuring stream nutrient concentrations and understanding longitudinal patterns in this highly modified watershed is important to better determine stream, canal, and nearshore ecosystem health. From July of 2018 to March of 2019, measurements of nutrients and environmental parameters were taken approximately monthly from thirteen sites along the three tributaries draining the Ala Wai Watershed. The Makiki Stream consistently registered elevated silicate, total phosphorus, and conductivity, suggesting a geological source. Samples from below Lyon Arboretum in the upper Mānoa Valley measured an increase of total organic nitrogen and ammonium. In the lower Mānoa Valley, the outflow water from Lo‘i o Kānewai taro patch was the most undersaturated in dissolved oxygen of the entire watershed while also exhibiting a drawdown of nitrate and nitrite with a concomitant increase in total organic nitrogen, total phosphorus, and ammonium concentrations. In the adjacent Pālolo Valley, an upstream tributary carried the highest concentration of total organic nitrogen, nitrate, and total phosphorus concentrations, consistent with agricultural practices and high-density onsite sewage disposal systems. A heavily channelized site near the lower stretches of Pālolo Stream exhibited the highest temperatures and concentrations of dissolved oxygen, pH, and ammonium in the system, highlighting the ecosystem impacts of waterway hardening. This study exposed the heterogeneity of nutrient and environmental parameter patterns in a relatively small watershed, demonstrating the value of longitudinal and time-series sampling to identifying nutrient sources, both natural and anthropogenic, between sites and streams. Future work investigating other streams should include high spatial and temporal resolution sampling to better understand intricate nutrient sources and sinks unique to those systems. Increased knowledge of the processes affecting the composition and concentrations of nutrients will aide in environmental management and policy making.

TABLE OF CONTENTS

ACKNOWLEDGEMENTS	ii
ABSTRACT	iii
LIST OF TABLES	v
LIST OF FIGURES	vi
1. INTRODUCTION	1
2. METHODS	3
2.1. Study Design	3
2.2. Site Selection and Sampling	4
3. RESULTS	5
3.1. Spatial Patterns	5
3.2. Temporal Patterns	8
4. DISCUSSION	10
4.1. Watershed Site Variability	10
4.2. Landscape Features	15
4.3. Event Response	18
5. CONCLUSION	18
APPENDIX	29
REFERENCES	32

LIST OF TABLES

Table 1. Sampling Dates and Times 20
Table 2. Sample Site Location Data 29
Table 3. Sampling Data 30

LIST OF FIGURES

Figure 1. Hawaiian Islands Map	21
Figure 2. Ala Wai Watershed Map	22
Figure 3. Box Plots of Environmental Parameters	23
Figure 4. Box Plots of TON, N+N, & Ammonium	24
Figure 5. Box Plots of TP, Orthophosphate, & Silicate	25
Figure 6. Color Contour Plots of Environmental Parameters.	26
Figure 7. Color Contour Plots of TON, N+N, & Ammonium	27
Figure 8. Color Contour Plots of TP, Orthophosphate, & Silicate	28

1. INTRODUCTION

Streams and rivers (lotic ecosystems) transport fresh water, sediments, nutrients, organic matter, contaminants, and debris downstream discharging into lakes, wetlands, estuaries, and ultimately the ocean, linking terrestrial processes with marine environments. Streams also support riparian ecosystems that affect the composition of the water and are dependent on upstream and adjacent processes as well as groundwater connectivity (Vannote et al., 1980; Walsh et al., 2005). As the human density of coastal and island communities grow, changes in land use result in modifications to waterways, including channelization for flood prevention and draining of floodplain estuaries. These modifications have often been made without consideration for the ecosystem health, resulting in negative perturbations with long-lasting impacts.

Nitrogen and phosphorus are key nutrients for stream biological production and are naturally present in organic and inorganic forms derived from soils and minerals; fixation and atmospheric deposition in the case of nitrogen; and both autochthonous and allochthonous detritus, and are transported into streams by groundwater, surface water runoff, and mass wasting (Kuypers et al., 2018; Paul and Meyer, 2001; Vannote, 1980; Vitousek et al., 1997; Walsh et al., 2005; Weigelhofer et al., 2018). Nitrogen or phosphorus can become a limiting nutrient if concentrations are too low. Conversely, increased concentrations of either can lead to nutrient pollution occurring through various mechanisms including the application of fertilizers, increased cultivation of nitrogen fixing crops, animal waste, effluent from onsite sewage disposal systems, rain deposition, and soil erosion (Kuypers et al., 2018; Paul and Meyer, 2001; USACE, 2015; Walsh et al., 2005). Nutrient loading disrupts the ecological balance of streams and can cause eutrophication (Vitousek et al., 1997; Weigelhofer et al., 2018; Whittier and El-Kadi, 2009). Consequences of eutrophication include anoxic conditions, reduced biodiversity, and harmful algae blooms (Vitousek et al., 1997; Weigelhofer et al., 2018).

Undisturbed streams and rivers have generalized, and predictable nutrient characteristics based on stream order (Vannote et al., 1980). Headwater streams, those with low stream orders, are often in steep terrain with low water volume, can be fast moving, and are frequently shaded by thick canopy vegetation; all reducing the photosynthetic potential and supporting a heterotrophic community metabolism. Nutrient concentrations are low and largely sourced from

allochthonous detritus producing a high organic to inorganic nutrient ratio (Vitousek et al., 1997; Weigelhofer et al., 2018). The high sediment surface area to water volume ratio allows for biogeochemical reactions at the sediment water interface to buffer nutrient concentrations limiting their downstream transport (Wymore et al., 2019). Downstream stretches have increased nutrient input from groundwater, surface runoff, and detritus. Instream and sedimentary biogeochemical reactions transform nutrient compositions decreasing the organic to inorganic nutrient ratio (De Carlo et al., 2004; Paul and Meyer, 2001). As rivers widen downstream, the shade from riparian vegetation decreases which in turn promotes increased photosynthesis and shifts community metabolism from heterotrophic to autotrophic, again further changing the nutrient composition (Rankin et al., 1999). The biogeochemistry of tropical volcanic island watersheds is dictated in part by the unique lithology and by the terrestrial ecosystem development of these systems (Chadwick et al., 1999; Chadwick et al., 2007). The weathering of basaltic lavas and volcanic ash plus the addition of organic material develop nutrient rich Andisols, Ustisols, and Vertisols soils; and fertile Mollisols and Inceptisols soils (Deenik and McClellan, 2007; Gavenda et al. 1998). Streams in these environments often remain low-order through their entirety due to the small watershed area retaining characteristics of headwater streams (Laws and Roth, 2004).

The Waikīkī area of O‘ahu in the Hawaiian Archipelago (Figure 1) was a natural wetland used for agriculture and aquaculture through the 19th century, with several loko i‘a (fishponds) and lo‘i kalo (wetland taro agriculture) where the present-day tourist district is located (Chan and Feeser, 2006). Construction of the Ala Wai Canal began in the beginning of the 20th century, with dredged material used to fill in the fishponds and wetlands. The canal functions as an estuary, receiving freshwater discharge from the streams and receiving sea water from the coastal ocean through tidal pumping. The Ala Wai Watershed, encompassing Waikīkī, is 42.4 square kilometers and drained by three streams: Makiki, Mānoa, and Pālolo (Figure 2). The Ko‘olau Range, rising to 930 meters in elevation above the Mānoa Valley, marks the upper boundary of the watershed. It has a steep slope with 75% of the elevation drop within 1.5 km of the ridge and 90% of the drop within 3 km. Streams on O‘ahu are subject to flash flooding, with annual rainfall in the upper watershed exceeding 380 cm annually (Giambelluca et al., 2013). Fifty-five percent of the watershed is classified as urban, 45% conservation, and less than 1% as

agricultural (Dashiell, 1997). The streams have been modified to prevent upland flooding and direct their discharge into the canal, consequently resulting in degraded ecosystem services such as reduced organic matter biodegradation, reduced removal of dissolved nutrients via sediment sorption and microbial activity, and reduced natural habitat (Paul and Meyer, 2001; Walsh et al., 2005). Trace metals measured in the Mānoa Stream by De Carlo et al (2004) provide evidence of fertilizer enrichment, and indicators of human sewage have previously been detected in the urban sector of the stream (Kirs et al., 2017). To understand mechanisms of nutrient inputs and transport in tropical stream ecosystems, which represent the primary conduits for nutrient pollution of coral reefs globally, there is a need for watershed-scale time series measurement of biogeochemical dynamics in modified urban habitats.

The intrusive stream alterations and increased urbanization of the Ala Wai Watershed have likely altered the nutrient compositions and concentrations within the streams. The goals of this study were to investigate and describe the nutrient concentration trends along the lengths of the Makiki, Mānoa, and Pālolo Streams; and to identify any possible nutrient enrichment sites or mechanisms. To reach these goals, longitudinal sampling of nutrients and water quality was conducted over a nine-month period of the three streams. The findings revealed a mosaic of anthropogenic stressors throughout the watershed contributing to the altered nutrient profiles.

2. METHODS

2.1. Study Design

One hundred and seven water samples and *in situ* measurements were taken from 13 sites across 10 dates on the Makiki, Mānoa, and Pālolo Streams in the Ala Wai Watershed. Samples were collected approximately monthly from July of 2018 through March of 2019 (Table 1). The sample sites were selected to represent stream endmembers, as well as neighboring tributaries, near stream or landscape features that were expected to influence water quality, and adjacent to continuous-record streamflow-gaging stations operated by the State of Hawai‘i Commission on Water Resource Management (CWRM) or United States Geological Survey (USGS) when possible.

2.2. Site Selection and Sampling

Thirty-two percent of Makiki stream has been altered, including hardened channels where the streambed and banks have been replaced by concrete; areas where the banks have been replaced or reinforced with revetments, but the bed remains; and culverts or conduits under roads or structures (Timbol and Maciolek, 1978). Two sites were selected on the Makiki Stream. The headwater site K1 (Figure 2) at 'CWRM station 3-115', was situated 3,575 meters from the Ala Wai Canal, and at an elevation of 115 m. The outflow site K2 (Figure 2) at 'USGS station 16238000' was 890 meters from the canal, and 4 m in elevation.

Twenty-four percent of Mānoa Stream (including Pālolo Stream) has been modified by lined channels, riparian vegetation removal and channel realignment, revetments, and culverts (Timbol and Maciolek, 1978). The Mānoa Stream had seven sample sites. The headwater site M1a (Figure 2) at 'CWRM station 3-114', was 7,700 meters from the canal, and 140 m in elevation, and upstream from the lower Lyon Arboretum grounds. Downstream of Lyon Arboretum was site M2a (Figure 2) at 'USGS station 16238500', 6,780 m from the canal, and 90 m in elevation. Site M1b (Figure 2) was along an adjacent tributary at 'USGS station 162240500', 6,770 m from the canal, and 90 m in elevation. The next sample site M3 (Figure 2) was after the convergence of the upper valley tributaries and midway down the Mānoa Valley at 'USGS station 16241600', 3,990 m from the canal, and 45 m in elevation. Farther down Mānoa Valley is Ka Papa Lo'i o Kānewai, a traditional Hawaiian taro patch. A small irrigation canal taps water from the Mānoa Stream to irrigate the lo'i and the return waters are subsequently routed back to Mānoa Stream. Site M4 (Figure 2) sampled water in the Mānoa Stream at the irrigation tap off, was 2,450 m from the canal, and 25 m in elevation. Site M5c (Figure 2) was 2,140 m from the canal, 20 m in elevation, and sampled the lo'i discharge water before it returned to the Mānoa Stream. The outflow site M6 (Figure 2) was at 'USGS station 16241600', 930 m from the canal, and 1 m in elevation.

The Pālolo Stream sampling sites began in two upper watershed tributaries which merge to form the Pālolo Stream. Two sites were sampled along the eastern tributary. The samples from these two sites never occurred on the same day so they were merged into one sample site to represent the tributary for analysis, P1a (Figure 2). The distances to the canal and elevations were averaged between these two sample locations resulting in 6,230 m and 136 m, respectively.

The next sample site, P1b (Figure 2) was along the western tributary located at ‘USGS 16244000’, 5,720 m from the canal, and 106 m in elevation. The lower Pālolo Stream site P2 (Figure 2) was sampled at ‘USGS 16247000’, 2,775 m from the canal, and 28 m in elevation. The Pālolo stream then merges with the Mānoa Stream and shares the same outflow to the canal after site M6.

In situ measurements of temperature, conductivity, dissolved oxygen (DO), and pH were made using a YSI ProDSS Multi-Parameter Water Quality Meter. Acid washed 500 ml polycarbonate bottles used for water samples were triple rinsed and submerged to 10 cm below the stream surface to collect whole water and immediately placed in a cooler with ice to be processed in the laboratory within six hours. Once in the laboratory, 45 ml of whole water was decanted into polypropylene centrifuge nutrient sampling tubes for total nitrogen (TN) and total phosphorus (TP) analysis and frozen to -20 °C. The remaining whole water was then peristaltically pumped through platinum or peroxide cured silicone tubing at a rate of 3 liters per hour. A small amount of water was flushed before pumping 100 ml through a 0.2 µm filter and discarded to clean the filter of plasticizers. Forty-five mL were pumped through the 0.2 µm filter into polypropylene centrifuge nutrient sampling tubes for dissolved nutrient analysis and frozen to -20 °C.

Water samples were processed at the University of Hawai‘i at Mānoa's SOEST Laboratory for Analytical Biogeochemistry (S-Lab) with the Seal Analytical AA3 HR Nutrient Autoanalyzer. Whole water samples were used for TN and TP. Filtered water samples were used for nitrate and nitrite (N+N), ammonium, orthophosphate, and silicate. Total organic nitrogen (TON) was derived by subtracting the inorganic nitrogen (N+N and ammonium) from TN.

3. RESULTS

3.1. Spatial Patterns

Temperature – The watershed's temperature geometric mean was 22.1 °C, and ranged from 18.3 °C to 31.1 °C. The Mānoa Stream temperature averaged 21.7 °C, ranging from 20.8 °C and 20.6 °C at the headwaters of M1a and M1b respectively, to 23.7 °C at the M6 outflow, an increase of 13.9% from M1a to M6 (Figure 3B). The temperature in Makiki Stream averaged 21.5 °C and ranged from 20.5 °C at K1 to 22.6 °C at K2 (Figure 3A). The mean temperature of

Pālolo Stream was 23.7 °C, with the headwater sites P1a and P1b averaging 21.4 °C and 22.2 °C, respectively. The highest mean temperature of the watershed was 27.7 °C at site P2 (Figure 3C).

Conductivity – The watershed's conductivity geometric mean was 183.6 $\mu\text{S cm}^{-1}$ and ranged from 90 $\mu\text{S cm}^{-1}$ to 415.8 $\mu\text{S cm}^{-1}$. The Mānoa Stream averaged 151.3 $\mu\text{S cm}^{-1}$, ranging from 119.4 $\mu\text{S cm}^{-1}$ at M1a and 129.3 $\mu\text{S cm}^{-1}$ at M1b to 206.4 $\mu\text{S cm}^{-1}$ at M6, an increase of 72.9% (Figure 3E). The Makiki Stream had the highest measured conductivity of the three streams with a geometric mean of 330.4 $\mu\text{S cm}^{-1}$ and ranged from 315.1 $\mu\text{S cm}^{-1}$ at K1 to 346.5 $\mu\text{S cm}^{-1}$ at K2 (Figure 3D). The mean conductivity of Pālolo Stream was 192.4 $\mu\text{S cm}^{-1}$. Its headwater sites differed from 119.3 $\mu\text{S cm}^{-1}$ at P1a and 208.7 $\mu\text{S cm}^{-1}$ at P1b and the stream conductivity increased to 249.2 $\mu\text{S cm}^{-1}$ at site P2 (Figure 3F).

Dissolved Oxygen – The watershed's DO geometric mean was 96.2% and ranged from 74.6% to 133%. The Mānoa Stream averaged 95.2% and ranged from 93.8% at M1a and 96.6% at M1b to 97.8% at M6. A drawdown of 1.4% was measured after Lyon Arboretum between sites M1a and M2a. A drawdown of 2.6% was measured in the lo'i between site M4 at 94.0% and site M5c at 91.4% (Figure 3H). The Makiki Stream's geometric mean for DO was 95.3% with little change from K1 at 95.5% to K2 at 95.1% (Figure 3G). The Pālolo Stream geometric mean was 99.1% and ranged from 95.5% at P1a and 92.8% at P1b to 111.3% at P2, the highest in the watershed, before mixing with the Mānoa Stream (Figure 3I).

pH – The pH geometric mean for the watershed was 7.40 and ranged from 6.04 to 9.79. The Mānoa Stream averaged 7.20 and ranged from 6.84 at M1a to 7.53 at M6 (Figure 3K). The Makiki Stream's pH averaged 7.90, ranging from 7.71 at K1 to 8.09 at K2 (Figure 3J). The Pālolo Stream's pH averaged 7.53 and ranged from 6.77 at P1a and 6.61 at P1b to 9.44 at P2 which was the highest mean pH throughout the watershed (Figure 3L).

Total Organic Nitrogen – The watershed's TON geometric mean was 6.20 μM , and ranged from 0.25 μM to 58.40 μM . The Mānoa Stream averaged 4.34 μM , ranging from 3.45 μM at M1a and 2.81 μM at M1b to 7.76 μM at M6. TON increased by 1.94 μM after Lyon

Arboretum from sites M1a to M2a. TON also increased by 2.03 μM after Lo‘i o Kānewai from site M4 to M5c (Figure 4B). The Makiki Stream averaged 6.03 μM , ranging from 5.52 μM at K1 to 6.59 μM at K2 (Figure 4A). The Pālolo Stream's geometric mean was 12.89 μM . Its headwaters averaged 7.52 μM at P1 and 28.63 μM at P1b, while P2 averaged 17.52 μM (Figure 4C).

Nitrate & Nitrite – The watershed N+N geometric mean was 5.24 μM , and ranged from 0.42 μM to 139.82 μM . The Mānoa Stream geometric mean was 4.07 μM , ranging from 0.97 μM at M1a to 7.25 μM at M6. A 3.5-fold increase was measured after Lyon Arboretum with a geometric mean of 3.43 μM at M2a. A drawdown of N+N after Lo‘i o Kānewai was measured from 8.41 μM at M4 to 5.07 μM at M5c (Figure 4E). The Makiki Stream geometric mean was 4.22 μM and ranged from 4.68 μM at K1 to 3.82 μM at K2 (Figure 4D). The Pālolo Stream geometric mean was 12.00 μM , and had contrasting means at the headwater sites, 2.76 μM at P1a and 46.17 μM at P1b, the highest of the watershed (Figure 4F).

Ammonium – The watershed's ammonium geometric mean was 0.22 μM and ranged from 0.02 μM to 6.96 μM . The Mānoa Stream averaged 0.22 μM and ranged from 0.09 μM at M1a to 0.50 μM at M6. A large increase was measured after Lyon arboretum at M2a with a geometric mean of 0.95 μM . An additional increase was measured after Lo‘i o Kānewai from 0.10 μM at M4 to 0.56 μM at M5c (Figure 4H). The Makiki Stream averaged 0.22 μM ranging from 0.2 at K1 to 0.25 μM at K2 (Figure 4G). The Pālolo Stream averaged 0.21 μM ranging from 0.12 at P1a and 0.07 at P1b to 0.98 μM at P2 (Figure 4I).

Total Phosphorus – The watershed's TP geometric mean was 0.70 μM , and ranged from 0.11 μM to 4.87 μM . The Mānoa Stream geometric mean was 0.43 μM and ranged from 0.23 μM at M1a and 0.55 μM at M1b to 0.56 μM at M6. The geometric mean nearly doubled after Lo‘i o Kānewai from 0.47 μM at M4 to 0.86 μM at M5c (Figure 5B). The Makiki Stream TP concentrations were the highest averaging 2.96 μM and ranged from 2.66 μM at K1 to 3.30 μM at K2 (Figure 5A). The Pālolo Stream averaged 0.79 μM with contrasting headwater values of

0.30 μM at P1a and 1.76 μM at P1b that mixed to an intermediate mean of 0.84 μM at P2 (Figure 5C).

Orthophosphate – The watershed's orthophosphate geometric mean was 0.42 μM , and ranged from 0.05 μM to 4.05 μM . The Mānoa Stream's average was 0.27 μM and ranged from contrasting headwater values of 0.10 μM at M1A and 0.18 μM at M2a to 0.41 μM at M6. An increase was measured after Lo‘i o Kānewai from 0.30 μM at M4 to 0.47 μM at M5c (Figure 5E). The Makiki Stream had the highest geometric mean at 2.00 μM and ranged from 1.89 μM at K1 to 2.12 μM at K2 (Figure 5D). The Pālolo Stream averaged 0.41 μM , and also had contrasting headwater values of 0.16 μM at P1a and 0.92 μM at P1b while P2 averaged 0.42 μM (Figure 5F).

Silicate – The watershed's silicate geometric mean was 184.7 μM , and ranged from 47.5 μM to 852.0 μM . The Mānoa Stream averaged 167.0 μM and ranged from 100.3 μM at M1a and 165.7 μM at M1b to 214.4 μM at M6 (Figure 5H). The Makiki Stream's silicate geometric mean was 281.6 μM and ranged from 271.1 μM at K1 to 292.4 μM at K2 (Figure 5G). The Pālolo Stream averaged 172.6 μM , ranging from 106.2 μM at P1a and 199.3 μM at P1b to 228.6 μM at P2 (Figure 5I).

3.2. Temporal Patterns

Temperature – The warmest average watershed temperatures occurred in August, September, and October of 2018, at 23.4, 23.5, and 23.3 °C, respectively. Cooling occurred throughout the watershed beginning in November of 2018, and stream waters reached their lowest temperatures in January of 2019 at a mean of 19.8 °C. Seasonal warming was first evident in February of 2019 at a mean of 21.3 °C and March of 2019 at a mean of 21.6 °C. (Figure 6A).

Conductivity – Conductivity decreased throughout the watershed from December of 2018 to January of 2019, from an average of 187.9 $\mu\text{S cm}^{-1}$ to 158.0 $\mu\text{S cm}^{-1}$ due to a precipitation

event that occurred during the January sampling. The conductivity increased in February of 2019 to an average of $196.3 \mu\text{S cm}^{-1}$ (Figure 6B).

Dissolved Oxygen – Dissolved oxygen did not show seasonal trends during the sampling period. A watershed-wide drawn down of the DO geometric mean was measured from 96.48 % in December of 2018 to 92.96 % in January of 2019 coinciding with the precipitation event in January (Figure 6C).

pH – There were no evident seasonal trends in pH during the sampling period. The pattern was remarkably stable throughout the watershed including the consistent increased values at site P2 on the Pālolo Stream (Figure 6D).

Total Organic Nitrogen – Low TON concentrations were measured in the Makiki and Mānoa Streams in November of 2018 averaging $2.75 \mu\text{M}$ and $2.06 \mu\text{M}$ respectively and the watershed's geometric mean was $3.53 \mu\text{M}$. A watershed-wide increase followed in December of 2018 to a mean of $13.95 \mu\text{M}$ (Figure 7A).

Nitrate & Nitrite – A drawdown of N+N concentrations occurred in December of 2018 with the watershed geometric mean decreasing from $7.00 \mu\text{M}$ in November of 2018 to $3.80 \mu\text{M}$ in December. The Pālolo Stream drawdown was greatest during this time from an average of $20.45 \mu\text{M}$ in November of 2018 to $3.64 \mu\text{M}$ in December of 2018 (Figure 7B).

Ammonium – The watershed-wide average ammonium concentrations increased from $0.175 \mu\text{M}$ in December of 2018 to $0.441 \mu\text{M}$ in January of 2019. In that same month, the geometric means of the Mānoa Stream sites M2a and M5c were $2.979 \mu\text{M}$ and $1.386 \mu\text{M}$, respectively and were notably higher than the total Mānoa Stream average of $0.403 \mu\text{M}$. Ammonium measured at the Pālolo Stream site P2 was $1.076 \mu\text{M}$, which was also higher than the stream's total geometric mean of $0.478 \mu\text{M}$ for the same month (Figure 7C).

Total Phosphorus – There were no discernable seasonal TP trends in the watershed. The largest change in the TP geometric mean was a decrease from 0.760 μM measured in August of 2018 to 0.534 μM measured in September of 2018. The greatest increase in the watershed TP geometric mean was from November of 2018 measured at 0.631 μM to 0.819 μM in December of 2018 (Figure 8A).

Orthophosphate – Similar to TP, orthophosphate seasonal trends were absent. Coinciding with the TP decrease from August to September of 2018, the watershed geometric mean of orthophosphate decreased from 0.530 μM to 0.373 μM . The change in orthophosphate from November to December of 2018 was opposite that of the TP increase. The orthophosphate geometric mean decreased from 0.444 μM in November to 0.314 μM in December of 2018 (Figure 8B).

Silicate – The average silicate concentration for the watershed was 228.1 μM in November of 2018 and increased to 246.9 μM in December of 2018. This increase was more prominent in the Makiki Stream increasing from a mean of 348.5 μM to 619.5 μM , along with increases in the lower Mānoa Stream from M3 through M6, as well as P2 in the Palolo Stream. The watershed's mean increased in January of 2019 to 324.6 μM , however the Makiki Stream average decreased by 40 μM but was offset by the increases in the Mānoa Stream of 44 μM , and the Pālolo Stream of 168 μM . Following the high watershed mean in January of 2019, concentrations decreased to a mean of 163.5 μM in February of 2019 (Figure 8C).

4. DISCUSSION

4.1. Watershed Site Variability

The temperature was lowest at the headwaters of all streams and gradually increased downstream (Figure 3), which is consistent with other studies on O‘ahu (Laws and Roth, 2004). The highest temperature of 31.1 °C recorded in the watershed at site P2 in the Pālolo Stream is only 0.9 °C less than the high temperature of 32.0 °C measured in the Waimānalo Stream by Laws and Roth (2004). The high temperatures measured at Pālolo and Waimānalo Streams were at stretches of heavily concreted channelization and riparian vegetation removal that would have

provided shaded. The water depths at both are low and spread across a wide flat bottom. These combined factors promote increased warming through solar insolation. Similar modifications have been made to several streams throughout O‘ahu (Laws and Roth, 2004; Timbol and Maciolek, 1978).

Conductivity was also lowest at the headwaters of each stream and increased downstream (Figure 3). The high conductivity measured at site P2 in the Pālolo Stream is associated with the increased temperatures and resulting evaporation increasing the ionic strength of the water. The conductivity geometric means for the Makiki, Mānoa, and Pālolo Streams were 330.4, 151.3 and 192.4 $\mu\text{S cm}^{-1}$, respectively. A study by Michaud and Wiegner (2011) investigated 24 streams on the island of Hawai‘i and found the geometric mean to be 66.1 $\mu\text{S cm}^{-1}$, with the highest stream measuring 123.9 $\mu\text{S cm}^{-1}$. The decreased conductivity values measured in the streams on the island of Hawai‘i are attributed to the younger geological age of the island, forming approximately 500-700 ka, where streams are mainly fed by surface runoff and submarine groundwater discharge is the main conduit for weathered ion transport to the ocean (Deenik and McClellan, 2007; Schopka and Derry, 2012). Erosional forces on older islands such as of O‘ahu, which formed approximately 2.2 Ma (Clague et al., 2016), have cut valleys and created groundwater pathways to feed stream baseflows, resulting in the greater groundwater influence on stream chemical composition (Schopka and Derry, 2012). Streams that support healthy and diverse biological communities range between 150 and 500 $\mu\text{S cm}^{-1}$ (Ellis, 1937) however, these values were established for continental rivers and streams in North America and do not consider geological timelines of volcanic islands. Although the geometric means of conductivity for this study fall within this defined range, it is more important to establish baseline values that can be used to identify anomalous measurements in the future and can aid in determining perturbations in the system.

Subsaturation of DO at the headwaters is expected in forested areas of low-order streams (Cummins, 1974; Rankin et al., 1999; Vannote, 1980) and the measurements of the three streams reflect that (Figure 3). Low light and quickly moving water suppress photosynthetic activity while increased respiration of allochthonous organic matter from plant litter consumes DO making the stream's metabolism heterotrophic. Downstream, the DO measurements remain relatively stable with two notable exceptions. First, site M5c in the Mānoa Stream which is just

downstream of the Lo‘i o Kānewai taro patch consisting of several flooded agricultural plots. The shallow-water system is characterized by low mixing and high organic matter, thus promoting oxygen consumption leading to anoxic conditions (discussed in the *Landscape Features Discussion* section). The second exception is site P2 in the Pālolo Stream, where DO was supersaturated. Concrete channelization of the stream and removal of shading plants prevents stream soil microbial respiration and allows high sunlight penetration, promoting algae growth and heightened photosynthesis (Cummins, 1974; Rankin et al., 1999). The reduction of dissolved carbon dioxide decreased the streams acidity, increasing the pH and indeed, site P2 had the highest pH measured in the watershed. Site P2 stands out as an anomaly transitioning from a heterotrophic system to an autotrophic system, one with increased DO and pH (Cummins, 1974). Similar conditions resulting in a metabolic shift to autotrophy in Waimānalo Stream were described by Laws and Roth (2004). Even though the DO is supersaturated along this stretch, the absolute concentration is limited by the increased temperatures, which can increase stress on the riverine biology.

The pH was lowest at the headwaters and increased downstream (Figure 3), consistent with Kāne‘ohe and Waimānalo Streams (Laws and Roth, 2004). The range of pH measured (6.04 – 9.79) was greater than a 2004 study of the Mānoa Stream where the range was 6.8 – 8.7 (De Carlo et al., 2004). The 2004 study only measured sites near M1b to M6 and therefore did not include sites near M1a on Mānoa Stream nor P2 on Pālolo Stream where the lowest and highest pH measurements were made for this study bringing attention to the importance of greater spatial sampling to understand the system more fully. The pH geometric means for the Makiki, Mānoa, and Pālolo Streams of 7.9, 7.2, and 7.5, respectively were similar to the geometric mean for the 24 Hawai‘i Island streams measured by Michaud and Wiegner (2011), which was 7.5.

TON was stable throughout each stream (Figure 4). The Makiki and Mānoa Streams had similar concentrations while Pālolo Stream was more enriched. Two sites on Mānoa Stream, M2a and M5c, along with P1b on Pālolo Stream had elevated concentrations compared to the watershed as a whole. This introduced higher TON concentrations into the Ala Wai Canal which could have had significant impacts on the estuarine and nearshore ecosystems. The TON measurements of this study compared well to dissolved organic nitrogen (DON) measurements of other streams studied on O‘ahu. Six O‘ahu streams were investigated in 2007 and divided into

three groups based on land type designation: conservation, agricultural, and urban with median DON values of 6.19, 17.89, and 9.36 μM , respectively (Hoover and Mackenzie, 2007). The median TON values of the Makiki, Mānoa, and Pālolo Streams in this study were 6.64, 4.92, and 12.19 μM , not surprisingly aligning more closely with conservation and urban groups of the 2007 study. The Pālolo Stream's slight increase may be from the influence of the small agricultural region in upper valley. Conversely, the TON values did not align with DON measurements from Hawai'i Island where the DON geometric mean for streams in conservation land was 2.91 μM and for streams running through agricultural regions was 1.06 μM (Michaud and Wiegner, 2011) well below the geometric means for the Ala Wai Watershed. The difference is explained by the geological age as older soils on O'ahu have had greater time to accumulate fixed atmospheric nitrogen; and increased groundwater influence on O'ahu streams as previously described (Michaud and Wiegner, 2011; Schopka and Derry, 2012).

Low N+N measurements were measured at both the M1a site of Mānoa Stream and the P1a site of Pālolo Stream (Figure 4). A sharp increase was measured from M1a to M2a across Lyon Arboretum, however site M1b adjacent to M2a (on a different tributary not influenced by the arboretum) has similar concentrations, indicating the increase is not attributed to the arboretum. Concentrations in Mānoa Stream slowly increase downstream apart from a drawdown at M5c (discussed in the *Landscape Features Discussion* section). Site P1b on Pālolo Stream had extremely high concentrations compared to all sites and caused the total Pālolo Stream N+N concentration geometric mean to increase. Regardless of this higher concentration, site M6 did not show a heightened concentration after the convergence of the Pālolo and Mānoa Streams. The Makiki, Mānoa, and Pālolo Stream's geometric means of N+N were 4.23, 4.07, and 10.30 μM which were comparable to the findings by Laws and Roth (2004) in Kāne'ohe Stream which was 7.65 μM . During the same 2004 study, the Waimānalo Stream's high geometric mean of 442.30 μM was attributed to dense livestock concentrations. The geometric means from the island of Hawai'i streams were 0.48 μM for conservation lands and 2.46 μM for agricultural lands, both lower than this studies values (Michaude and Wiegner, 2011). Hoover and Mackenzie (2009) reported the median N+N values for O'ahu conservation streams to be 3.25 μM , agricultural streams to be 11.92 μM , and urban streams to be 9.49 μM . These values align well with the Makiki Stream median at 4.31 μM , Mānoa Stream at 4.93 μM , and Pālolo Stream

at 10.95 μM . Puerto Rico offers a comparison to an older volcanic island. Luquillo Experimental Forest (LEF) is a National Science Foundation's Long Term Ecological Research (LTER) site situated in eastern Puerto Rico with most volcanic formations 105 to 85 million years old (Ma) and some as young 42 Ma (Murphy et al., 2012). A study at LEF investigated three streams and reported a collective N+N geometric mean of 1.28 μM (Brereton, 2017), consistent with older and more developed tropical habitats becoming more nutrient retentive. The increased values reported on O'ahu exemplified the relative younger age of the island and forest landscapes.

All headwater sites had lower ammonium concentrations (Figure 4). A significant increase along the Mānoa Stream was measured from sites M1a to M2a across Lyon Arboretum but the concentration was not sustained downstream as it was diluted from mixing with the other highland tributaries indicating Lyon Arboretum as the point source. A decreasing trend was noted in the Mānoa Stream until a second sharp increase was measured at site M5c. Similarly, the Pālolo Stream's low headwater concentrations rose significantly at site P2. The increased ammonium concentrations from Pālolo Stream and at M5c of Mānoa Stream could have contributed to eutrophication in the estuarine canal system. The medians of ammonium concentrations for the Makiki, Mānoa, and Pālolo Streams were 0.23, 0.22, and 0.39 μM , respectively, comparing well to streams on O'ahu conservation lands reported by Hoover and Mackenzie (2009) at 0.3 μM , whereas agricultural and urban streams medians were measured at 4.22 and 2.22 μM , respectively, suggesting the upland conservation areas in the Ala Wai Watershed have a greater influence over the stream compared to the urban sectors. Most measurements for the study on the island of Hawai'i were below detection (Michaude and Wiegner, 2011). The Puerto Rico LEF study reported a geometric mean of 0.47 μM (Brereton, 2017) comparable to Ala Wai Watershed streams.

Total Phosphorous and orthophosphate have similar general trends in all three streams, slightly increasing from headwaters to outflow (Figure 5). The Mānoa and Pālolo Streams are comparable to others on O'ahu, Hawai'i Island, and Puerto Rico while the concentrations throughout Makiki Stream are anomalously high. In the Mānoa Stream, elevated concentrations in both TP and orthophosphate were measured at site M1b. A notable increase was measured at M5c of both TP and orthophosphate (discussed in the *Landscape Features Discussion* section). Site P1a along the Pālolo Stream had lower concentrations in both TP and orthophosphate while

P1b was heightened in both. There was little change after the two Pālolo tributaries merged nor after the convergence of Pālolo and Mānoa Streams. The slightly elevated concentration measured at M6 as compared to the head water sites of M1a and P1a was due to the increased concentrations from M1b, M5c, and P2. The median orthophosphate for Makiki Stream was 1.93 μM , Mānoa Stream was 0.29 μM , and Pālolo Stream was 0.42 μM , while the O‘ahu streams reported by Hoover and Mackenzie (2009) were 0.29 μM for conservation lands, 0.39 μM for agricultural lands, and 0.57 μM for urban lands. The orthophosphate geometric means in this study were 2.00 μM for Makiki Stream, 0.27 μM for Mānoa Stream, and 0.41 μM for Pālolo Stream, while most measurements made during the Hawai‘i Island study were below detection but of those above were in the agricultural regions and reported a 0.21 μM geometric mean (Michaude and Wiegner, 2011). The LEF LTER study in Puerto Rico measured an orthophosphate mean of 0.47 μM (Brereton, 2017).

Silicate concentrations are from groundwater mobilizing silicate in the soil (Hoover, 2002). The concentrations in the Mānoa and Pālolo Streams were lowest at the headwaters and increased slightly downstream (Figure 5). The geometric means for Makiki, Mānoa, and Pālolo Streams were 281.6, 167.0, and 184.3 μM , respectively, lower than Kāne‘ohe Stream reported at 362.6 μM and more similar to Waimānalo Stream reported at 227.8 μM (Laws and Roth, 2004), possibly due to the unique variabilities among streams on O‘ahu.

4.2. Landscape Features Discussion

Makiki Stream – The Makiki Stream had anomalously high conductivity, TP, and orthophosphate measurements compared to the other two streams and is likely due to the unique geological history of the Makiki sub watershed, the density of onsite sewage disposal systems (OSDS), or a combination of the two. The Makiki Stream runs through Mount Tantalus, an area that was volcanically active during the rejuvenated stage volcanism on O‘ahu with the last eruption approximately 76 ka which produced a one-meter-thick ash field over much of Mount Tantalus and is covered by one meter of soil today (Clague et al., 2016). The Makiki and Mount Tantalus regions also have a high density of OSDS reaching levels that are a significant potential threat to groundwater as deemed by the Environmental Protection Agency (Whittier and el-Kadi, 2009). The ash field and OSDS are both possible candidates for the cause of the Makiki Stream

pH, TP, and orthophosphate anomalies, however, OSDS leaching would also produce increased nitrogen concentrations which were not identified.

Lyon Arboretum – The Mānoa Stream site M1b is downstream of Lyon Arboretum. Agricultural practices and processes in the arboretum are responsible for the differences measured between M1a and M1b. TON, N+N, and ammonium - all have high slope increases between these two sites. As mentioned earlier however, the N+N concentration measured at M1b was similar to M2a, it's neighboring site on a different tributary stream. Thus, the increase of N+N measured at M1b was likely not due to the arboretum but a natural increase in the upper watershed. In contrast, the increase of TON and ammonium concentrations were unique and likely caused by the arboretum. Possible causes are relict cesspools and active mulching (Group 70 International, INC., 2005). Fertilizing is used periodically but very limited. The lack of significant increase in phosphorus concentrations also suggests that fertilizers were not the cause for increased TON and ammonium. Active mulching and the breakdown of this organic matter is therefore the most plausible explanation for these increases.

Lo'i o Kānewai – Lo'i o Kānewai taro patch is located between the Mānoa Stream sites M4 and M5c. M5c is downstream of the lo'i and upstream of the return to Mānoa Stream so that measurements taken there show changes occurring in the lo'i. The lo'i consists of several flooded agriculture patches used for taro cultivation. The central area is cleared of trees to allow sun light penetration. The flooded patches maintain standing water and through the respiration of organic matter, dissolved oxygen decreases. Depending on the extent of this respiration, suboxic and anoxic conditions near the sediment-water interface can occur. DO concentrations at site M5c were lower than M4 suggesting that this process was taking place. In anoxic conditions, heterotrophic bacteria utilize other electron acceptors in place of oxygen in a series of redox reactions based on thermodynamic favorability. The most favorable after oxygen is nitrate which is evident at the lo'i as N+N concentrations at M5c were less than M4. The fate of the nitrate can either be conversion to nitrogen gas and subsequent loss to the atmosphere, or conversion to ammonium through dissimilatory nitrate reduction (Kraft et al., 2014; Kuypers et al., 2018), a possibility in the lo'i as ammonium concentrations increased significantly. Additionally, the increase in orthophosphate at M5c gave further evidence of anoxic conditions and redox reactions taking place. After nitrate and manganese, the next energetically favorable electron

acceptor is Fe(III). As Fe(III) is reduced to Fe(II), phosphate bound to Fe(III) is released as dissolved ions, fluxing upwards toward the sediment-water interface, where two possibilities exist: either 1) phosphate ions are re-scavenged by Fe(II) oxidizing to Fe(III) in the oxic conditions above the sediment-water interface resulting in a phosphorus sink, or 2) Fe(II) binds with sulfides, precipitating out of the water column, and allowing phosphate ions to remain dissolved and available for biotic uptake or transport downstream (Chambers and Odum, 1990; Mortimer, 1941; Parsons et al., 2017). A major consideration is that soils in Hawai‘i are enriched in iron presenting a strong potential for binding with phosphate, limiting phosphate ion concentration in streams (Bruland and DeMent 2009; Chambers and Odum, 1990). Other confounding variables include concentrations of organic matter in the soil, pH, and porewater transport (Bruland and DeMent 2009; Chambers and Odum, 1990). Nonetheless, the measured increase in orthophosphate at site M5c suggests that processes in the lo‘i are freeing phosphate ions and allowing their transport downstream.

Upper Pālolo Tributary – Site P1b on the wester tributary to the Pālolo Stream has heightened TON, N+N, TP, and orthophosphate concentrations, much higher than the other headwaters in the Pālolo and Mānoa Streams. Additionally, it is also the only region of the Ala Wai Watershed classified as agricultural lands (De Carlo and Anthony, 2002). These increased concentrations are likely from compost and fertilizer application but also may be due to OSDS leaching.

Pālolo Concrete Channelization – Site P2 on the lower Pālolo Stream is along a section of heavy modification including wide concrete channelization of both the walls and streambed, and the removal of riparian vegetation that would have provided shade. In addition to the increased temperature, conductivity, DO, and pH discussed prior there is a measured increase in ammonium concentrations which may be caused by the decay of algae. An abnormally thick algae mat was noted when the highest ammonium concentration (3.03 μM) was measured at site P2.

Evidence suggests that the Makiki Stream nutrient composition is predominantly influenced by relatively young volcanism on Mount Tantalus, and to a degree, the density of onsite sewage disposal systems. The Mānoa Stream composition is moderated by the upstream addition of TON and ammonium from Lyon Arboretum; and the lo‘i contributing to increased

concentrations of TON, ammonium, TP, and orthophosphate while reducing the N+N concentrations through redox reactions. The Pālolo Stream's composition is moderated by agricultural practices and/or OSDS leaching in the upper valley contributing to increased TON, N+N, TP, and orthophosphate concentrations; and the channelization of Pālolo Stream contributing to increased ammonium as well as heat.

4.3. Event Response

The 9-month sampling time span, from July of 2018 to March of 2019, limits any seasonality conclusions from this study, regardless, no seasonality trend was identified. A multi-year study would be needed to draw robust conclusions about seasonal trends. Moreover, sampling approximately monthly in a system prone to flash flooding would introduce under-sampling errors (Tomlinson and De Carlo, 2003). Sampling on January 26th, 2019 coincided with the end of a storm and although discharge was well below the peak it remained above base flow at some sites. Temperature measurements were lower at all sites in the watershed and concurrent increases in stream flow resulted in decreased conductivity. There was no conclusive change in nitrogen or phosphorus due to the increased flow which may be explained by a lack of temporal sampling resolution. Counterintuitively, silicate did seem to increase throughout much of the watershed. Dissolved silicate concentrations are greatest when groundwater has enough time to reach or approach equilibrium with the surrounding soils. During a storm, surface soils with lower silicate concentrations become super saturated and together with surface runoff, the stream silicate concentrations would be expected to become diluted (Hoover, 2002). This point is of course comparing measurements a month apart and the rise in dissolved silicate may be an artifact from the lack of temporal resolution.

5. CONCLUSION

Through this investigation of the Ala Wai Watershed, nutrient trends in the Makiki, Mānoa, and Pālolo Streams were measured and described. Upper watershed sites near Lyon Arboretum and agriculture lands in the upper Pālolo watershed were identified as possible sources of headwater nutrient enrichment. Although some increases in headwater nutrient concentrations appear inconsequential downstream due to dilution from converging tributaries,

the functional health of the downstream components and discharge into the canal are dependent to a degree on the headwater quality (Rankin et al., 1999; Vannote, 1980) and should not be ignored. A heavily modified stretch of the Pālolo Stream was shown to transition from a heterotrophic to autotrophic stream metabolism, altering nitrogen species concentrations. Lo‘i o Kānewai along the Mānoa Stream exhibited suboxic conditions promoting redox reactions altering nitrogen species and increasing orthophosphate ion availability. The Makiki Stream had the highest concentrations of TP and orthophosphate along with heightened conductivity likely from its unique geological history.

The majority of the measurements made in this study agree well with previous studies of streams on O‘ahu. The Mānoa and Pālolo Stream silicate measurements were lower in this study compared to other O‘ahu streams which may be explained by localized variability. Conductivity, TON, N+N, ammonium, and orthophosphate measurements were greater than streams on the island of Hawai‘i, as is expected due to the relatively young age of Hawai‘i Island and the lack of groundwater connectivity to surface streams. N+N concentrations were greater than streams sampled in Puerto Rico, again as expected as older, more developed forests increase nutrient retention, however ammonium and orthophosphate concentrations were comparable. These comparisons highlight the importance of geological age of islands, as well as maturity of forested regions on the water quality of streams.

Although this study investigated nutrient concentrations during predominantly low-flow conditions, low-flow nutrient fluxes into the canal are not described. Future work can use the available USGS discharge data for the watershed in conjunction with the baseflow measurements described here to build a terrestrial derived nutrient budget for the canal. Including high-flow conditions measurement, submarine groundwater flux, and urban runoff not accounted for in the streams would provide a complete nutrient budget to the Ala Wai Canal from the watershed which would be useful for future canal and nearshore studies, management and policy decisions, and upstream mitigation strategies.

Table 1. Sampling dates and times for each site. Time is Hawaiian Standard Time

		Jul 3 rd , 2018 08:40-10:00	Aug 3 rd , 2018 09:20-13:30	Aug 22 nd , 2018 17:00-18:58	Sep 9 th , 2018 08:36-14:36	Oct 13 th , 2018 08:20-12:50	Nov 24 th , 2018 08:18-12:22	Dec 15 th , 2018 08:08-13:08	Jan 26 th , 2019 08:25-14:08	Feb 23 rd , 2019 08:21-13:49	Mar 23 rd , 2019 08:32-12:34
Makiki	K1	•	•	•	•	•	•	•	•	•	•
	K2	•	•	•	•	•	•	•	•	•	•
Mānoa	M1a	•*	•	!	•	•	•	•	•	•	•
	M2a	•	•	!	•	•	•	•	•	•	•
	M1b	•	•	!	•	•	•	•	•	•	•
	M3	•*	•	!	•	•	•	•	•	•	•
	M4	•	•	!	•	•	•	•	•	•	•
	M5c	•	•	!	•	•	†	•	•	•	•
	M6	•*	•	•	•	•	•	•	•	•	•
Pālolo	P1a	•	•	!	•	•	•	•	•	•	•
	P1b	•	•	!	•	•	•	•	•	•	•
	P2	•	•	•	•	•	•	•	•	•	•

- Sample collected
- * Three samples collected, and the mean was reported
- ! Samples not collected due to approaching hurricane
- † Low flow prevented sampling

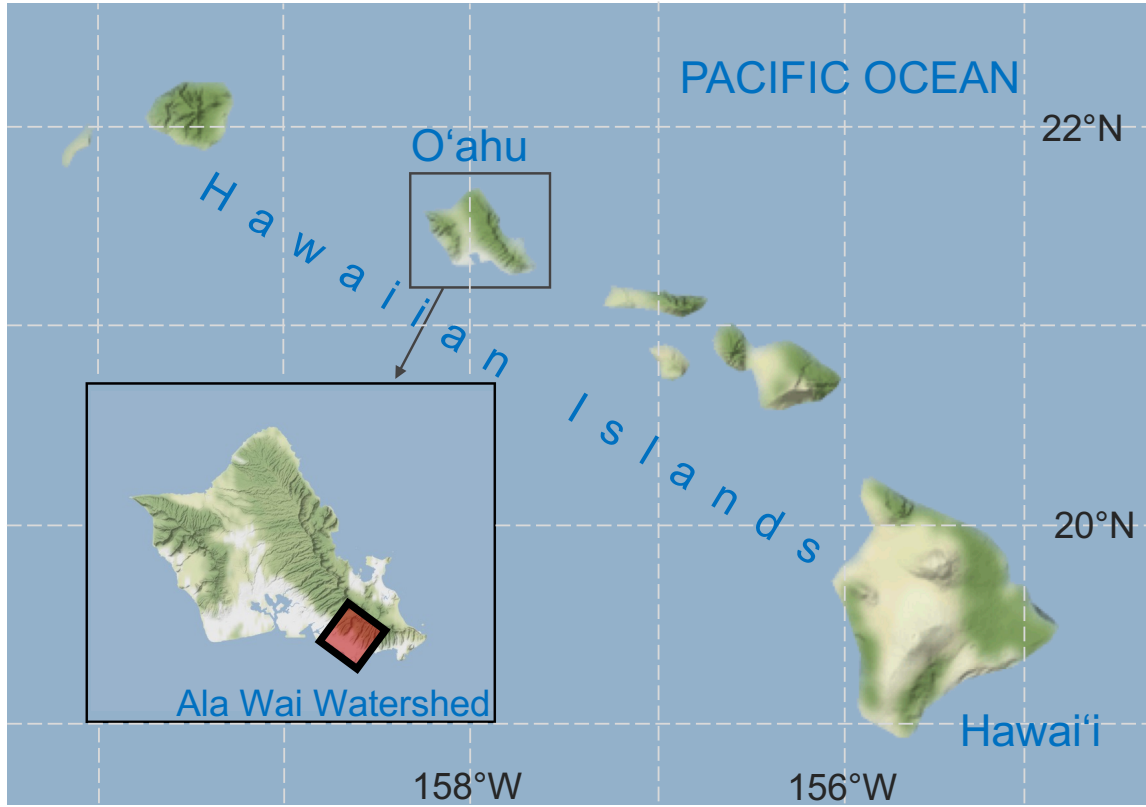


Figure 1. The Main Hawaiian Islands with the black box showing the island of O'ahu. The red highlight box indicates the Ala Wai Watershed.



Figure 2. The Ala Wai Watershed. The dashed yellow line is the watershed boundary. The green highlighted streams show the Makiki Stream and its tributaries along with sample sites K1 and K2. The blue highlighted streams show the Mānoa Stream and its tributaries with sample sites M1a, M2a, M1b, M3, M4, M5c, and M6. The pink highlighted streams show the Pālolo Stream and its tributaries with sample sites P1a, P1b, and P2. The Ala Wai Canal is highlighted in orange. White filled circles show Lyon Arboretum and Ka Papa Lo'i o Kānewai.

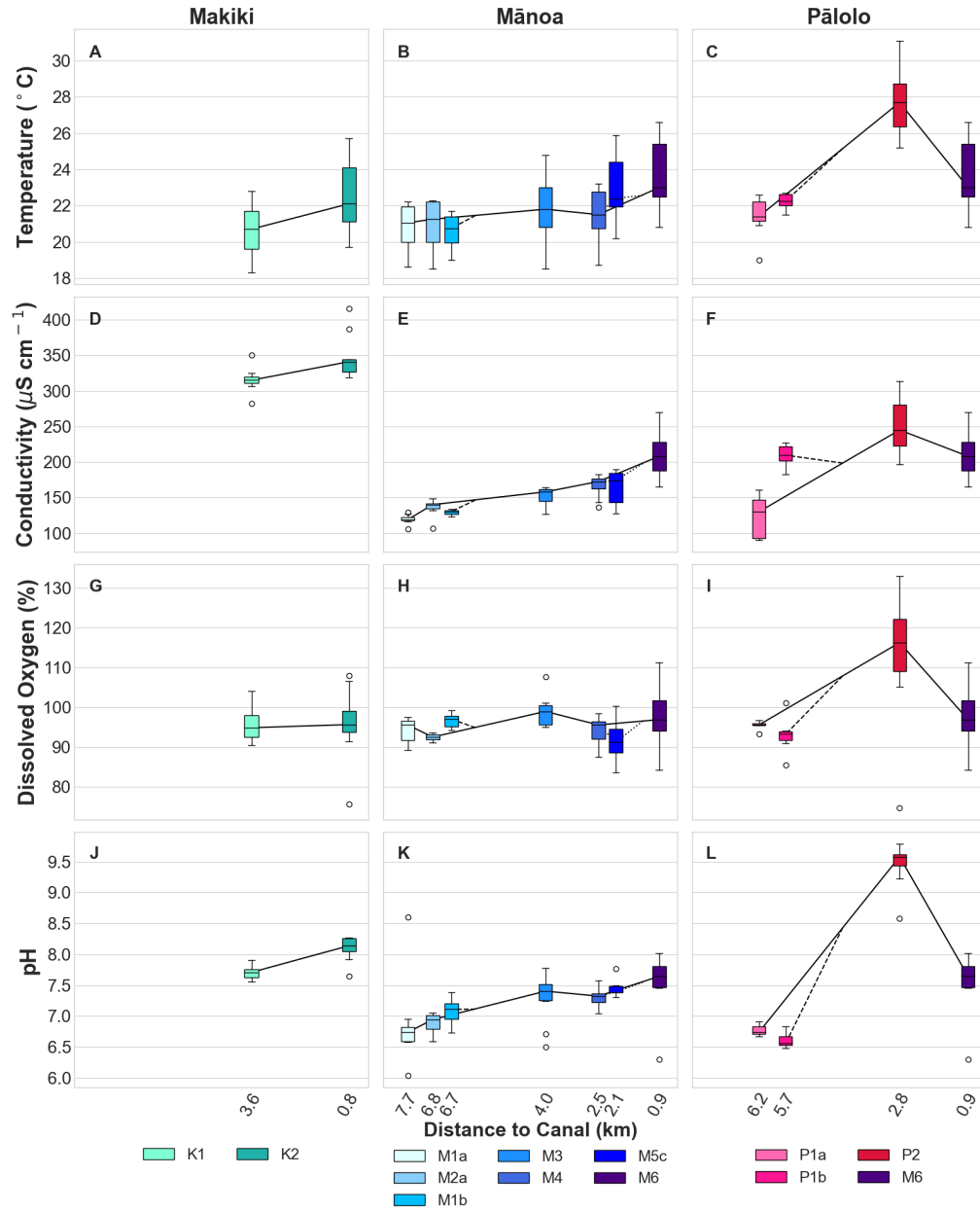


Figure 3. Environmental parameters measured in situ displayed as box plots for each site. The subplots are divided by stream from left to right: Makiki, Mānoa, and Pālolo. Boxplots show minimum, maximum, median, first quartile, third quartile, and outliers for each site. Within each subplot the solid interconnected lines from left to right show the flow of the stream from headwaters towards the canal and are connected to the median values at each sampling site. Dashed lines from M1b in Mānoa Stream and P1b in Pālolo Stream represent tributaries merging into the streams. The dotted line to and from M5c represents a diversion from Mānoa Stream into Lo'i o Kānewai taro patch and return to Mānoa Stream. The vertical axes are temperature (°C): A – C; conductivity ($\mu\text{S cm}^{-1}$): D – F; dissolved oxygen (%): G – I; and pH: K – L.

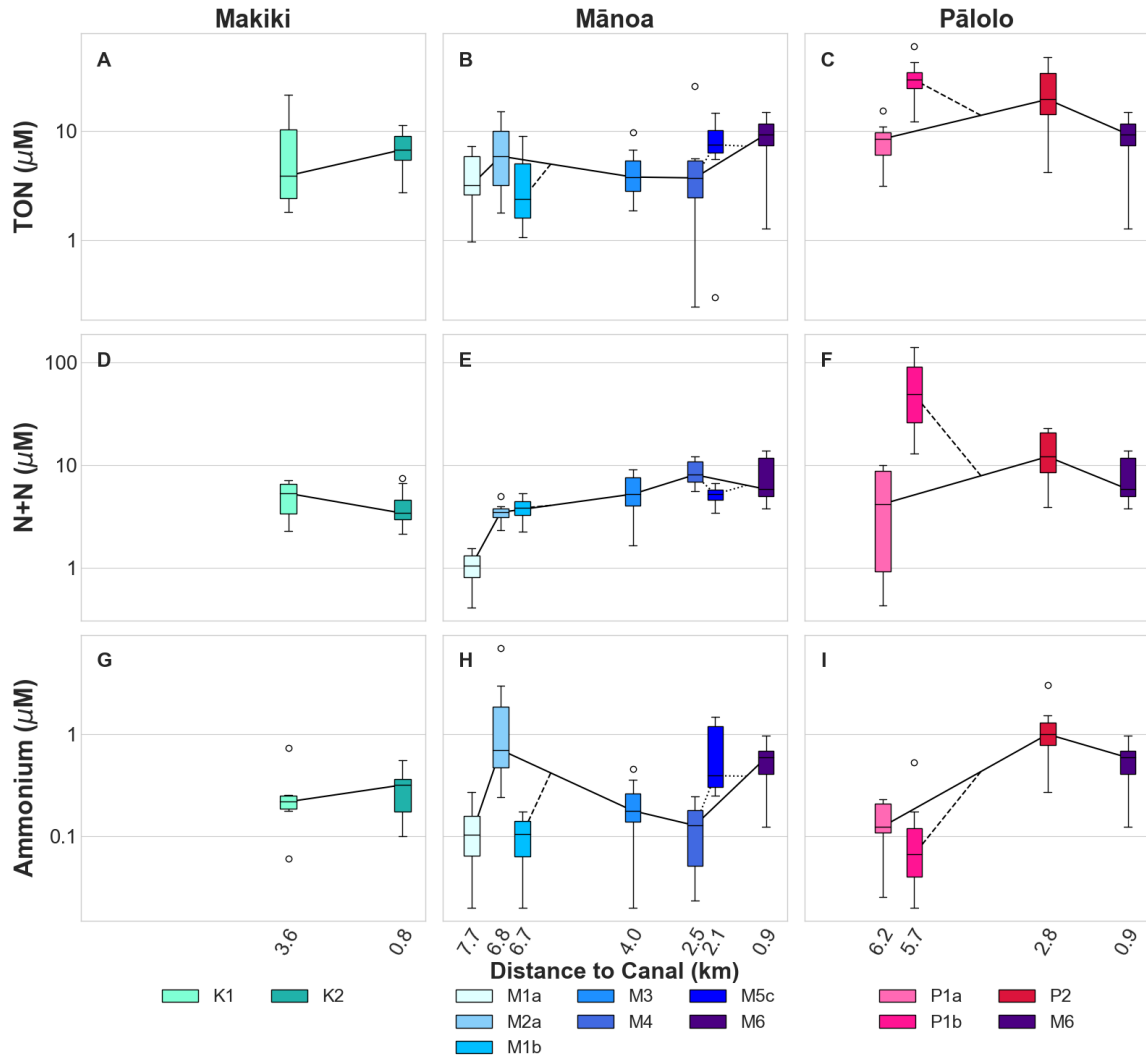


Figure 4. Nutrient concentrations shown as box plots. The subplots are divided by stream from left to right: Makiki, Mānoa, and Pālolo. Boxplots show minimum, maximum, median, first quartile, third quartile, and outliers for each site. Within each subplot the solid interconnected lines from left to right show the flow of the stream from headwaters towards the canal and are connected to the median values at each sampling site. Dashed lines from M1b in Mānoa Stream and P1b in Pālolo Stream represent tributaries merging into the streams. The dotted line to and from M5c represents a diversion from Mānoa Stream into Lo'i o Kānewai taro patch and return to Mānoa Stream. The vertical axes are total organic nitrogen (μM): A – C; nitrate & nitrite (μM): D – F; ammonium (μM): G – I and are log base 10 scale.

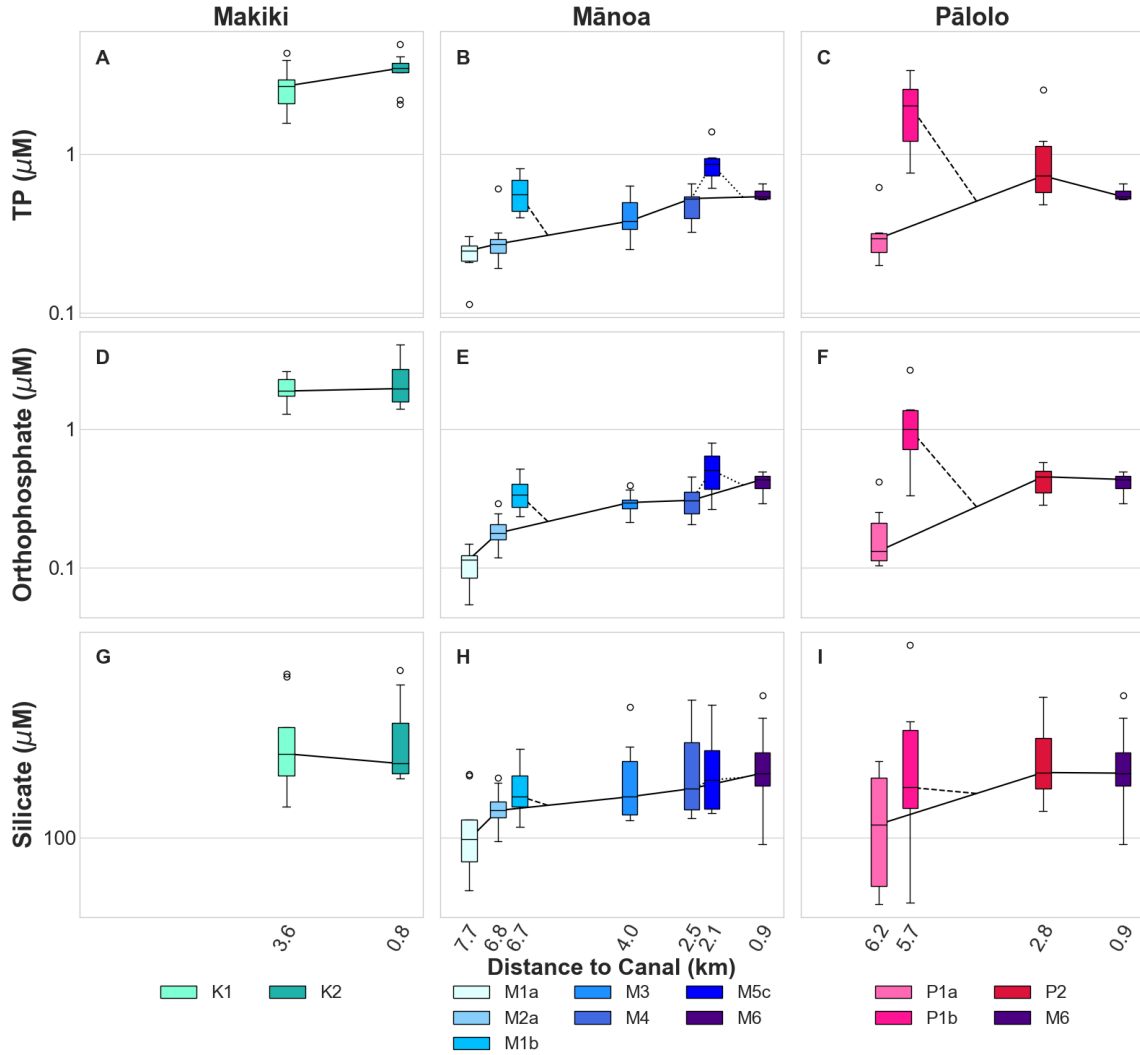


Figure 5. Nutrient concentrations shown as box plots. The subplots are divided by stream from left to right: Makiki, Mānoa, and Pālolo. Boxplots showing minimum, maximum, median, first quartile, third quartile, and outliers for each site. Within each subplot the solid interconnected lines from left to right show the flow of the stream from headwaters towards the canal and are connected to the median values at each sampling site. The solid interconnected lines from left to right show the flow of the stream from headwaters towards the canal and are connected to the median values at each sampling site. Dashed lines from M1b in Mānoa Stream and P1b in Pālolo Stream represent tributaries merging into the streams. The dotted line to and from M5c represents a diversion from Mānoa Stream into Lo'i o Kānewai taro patch and return to Mānoa Stream. The vertical axes are total phosphorus (μM): A – C; orthophosphate (μM): D – F; silicate (μM): G – I and are in log base 10 scale.

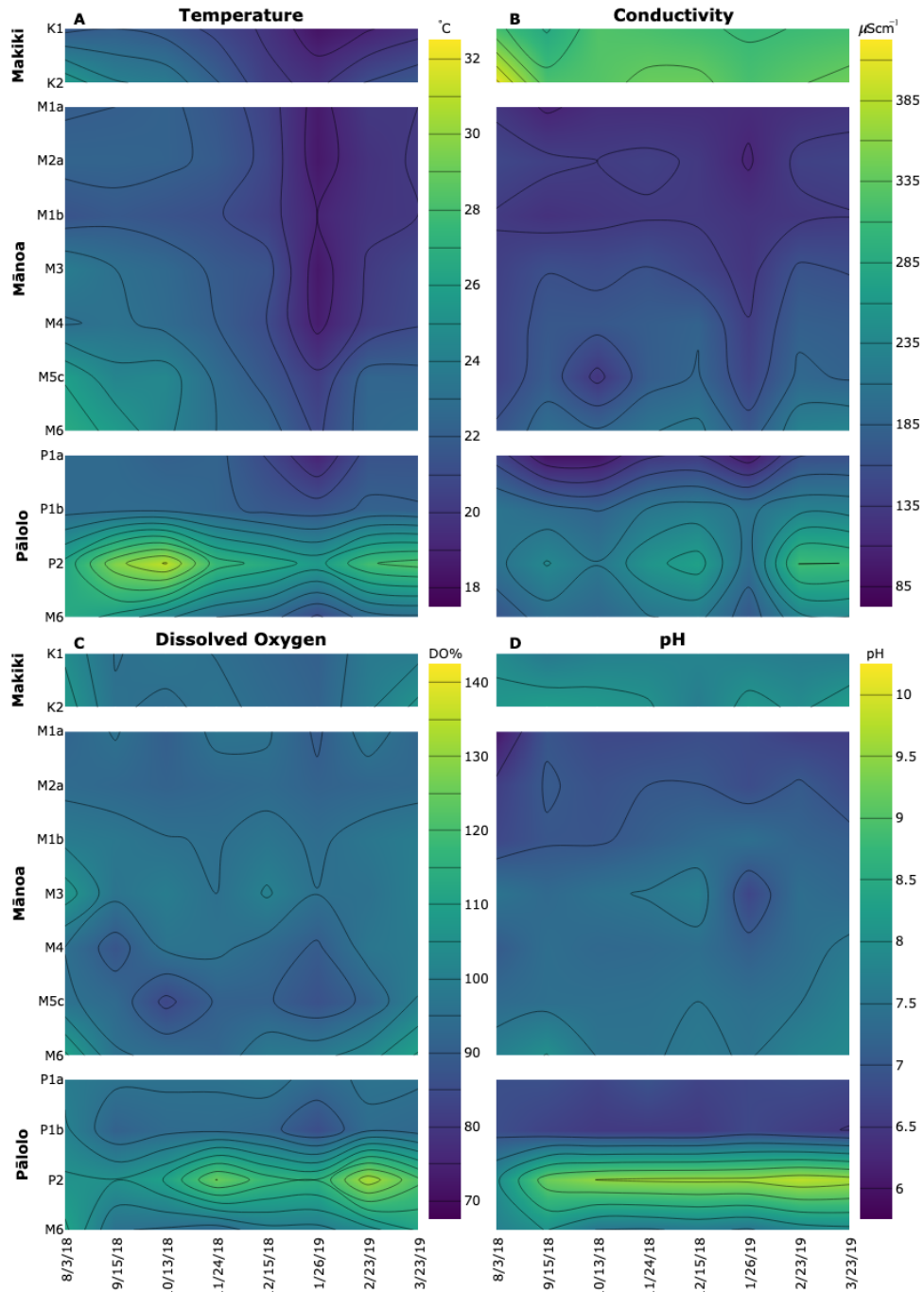


Figure 6. Environmental parameter color contour subplots divided by streams from top to bottom: Makiki, Mānoa, and Pālolo. The horizontal axis is the date of sampling, and the vertical axis is sampling sites from headwaters at the top to outflow at the bottom for each stream. The color bars show the scale for each parameter; **A**: temperature ($^{\circ}\text{C}$); **B**: conductivity ($\mu\text{S cm}^{-1}$); **C**: dissolved oxygen (%); and **D**: pH. Samples taken on July 31st and August 22nd, 2018 were removed from the seasonal analysis as less than 50% of stations were sampled on those days.

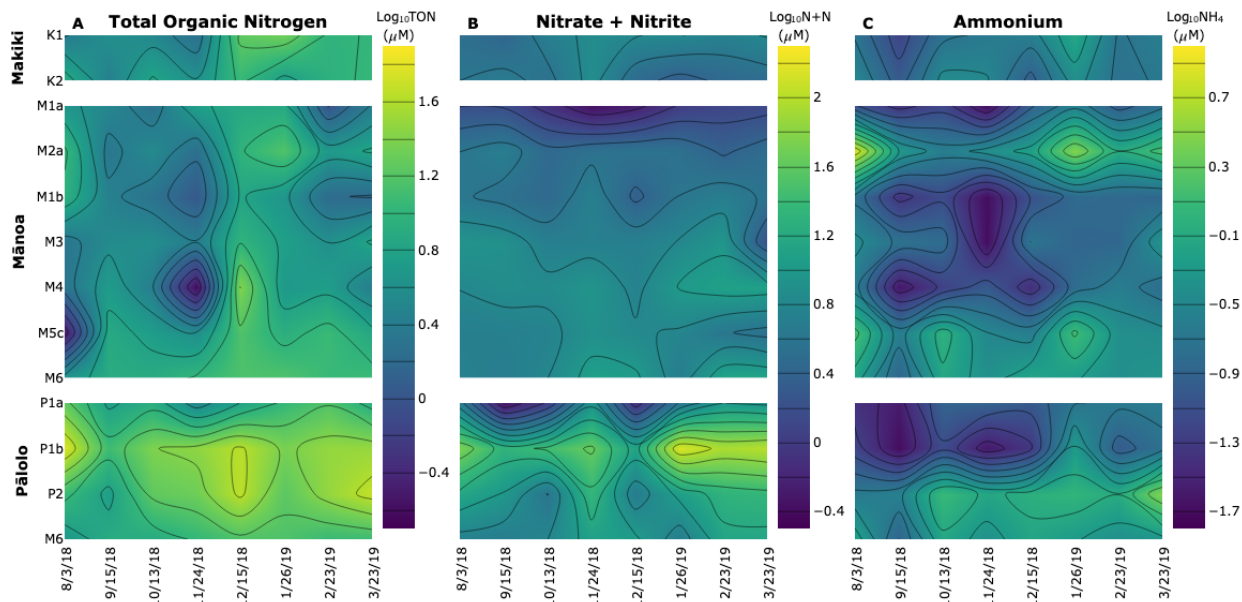


Figure 7. Nutrient concentration color contour subplots divided by streams from top to bottom: Makiki, Mānoa, and Pālolo. The horizontal axes are the sampling dates, and the vertical axes are sampling sites from headwaters at the top to outflow at the bottom for each stream. The color bars show the scale for each parameter which have been log base 10 transformed and are in μM ; **A**: total organic nitrogen; **B**: nitrate & nitrite; **C**: and ammonium. Samples taken on July 31st and August 22nd, 2018 were removed from the seasonal analysis as less than 50% of stations were sampled on those days.

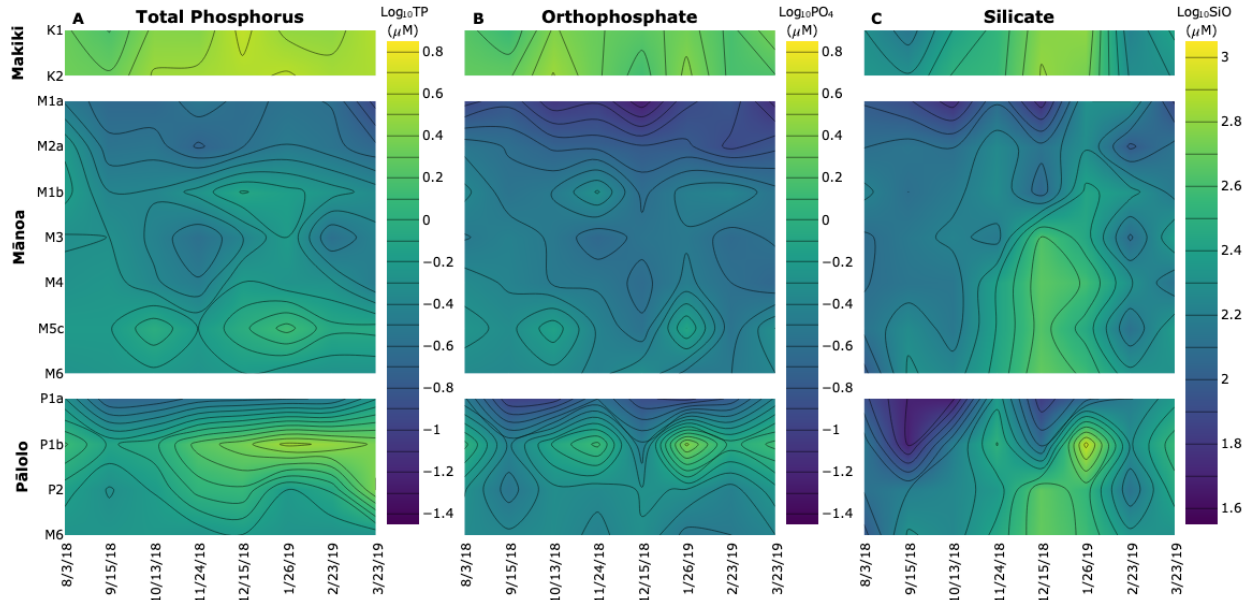


Figure 8. Nutrient concentration color contour subplots divided by streams from top to bottom: Makiki, Mānoa, and Pālolo. The horizontal axes are the sampling dates, and the vertical axes are sampling sites from headwaters at the top to outflow at the bottom for each stream. The color bars show the scale for each parameter which have been log base 10 transformed and are in μM ; **A**: total phosphorus; **B**: orthophosphate; and **C**: silicate. Samples taken on July 31st and August 22nd, 2018 were removed from the seasonal analysis as less than 50% of stations were sampled on those days.

APPENDIX

Table 2. Sample site location data. Distance is measured from the Ala Wai Canal. Distance and elevation are in meters.

Site	Stream	Latitude	Longitude	Distance	Elevation
K1	Makiki	21.317994	-157.82688	3575	115
K2	Makiki	21.297088	-157.836726	890	4
M1a	Mānoa	21.334077	-157.801792	7700	140
M2a	Mānoa	21.328339	-157.80083	6780	90
M1b	Mānoa	21.327906	-157.799514	6770	90
M3	Mānoa	21.308471	-157.809433	3990	45
M4	Mānoa	21.297491	-157.813809	2450	20
M5c	Mānoa	21.29517	-157.812522	2140	20
M6	Mānoa	21.287291	-157.818039	930	1
WOU	Pālolo	21.312219	-157.780954	6825	170
WOCM	Pālolo	21.303281	-157.785423	5635	101
P1b	Pālolo	21.306671	-157.788326	5720	106
P2	Pālolo	21.289275	-157.804612	2775	28

Table 3. Sample data. Time is Hawaiian Standard Time; Temp: temperature (°C); DO: dissolved oxygen (%); Cond: conductivity ($\mu\text{S cm}^{-1}$); TN: total nitrogen (μM); TP: total phosphorus (μM); PO4: orthophosphate (μM); SiOx: dissolved silicate (μM); N+N: nitrate and nitrite (μM); NH4: ammonium (μM).

Date	Time	Site	Temp	DO	Cond	pH	TN	TP	PO4	SiOx	N+N	NH4
7/3/18	8:40	M1a		97		8.60	4.4	0.25	0.12	110	1.06	0.16
7/3/18	9:19	M3		101		6.50	7.7	0.52	0.39	123	3.65	0.28
7/3/18	10:00	M6		94		6.30	13.5	0.65	0.48	158	5.29	0.97
8/3/18	12:07	K1	21.7	104	317	7.91	6.0	2.08	1.73	202	3.40	0.19
8/3/18	12:45	K2	25.7	108	416	8.11	12.3	2.18	1.95	217	3.98	0.32
8/3/18	9:20	M1a	21.9	92	130	6.04	6.2	0.30	0.11	98	1.56	0.08
8/3/18	9:50	M2a	22.3	94	149	6.59	21.8	0.60	0.29	125	3.98	6.96
8/3/18	10:10	M1b	21.4	99	133	6.73	13.3	0.69	0.43	168	4.26	0.18
8/3/18	10:30	M3	23.8	108	140	7.48	11.1	0.49	0.31	121	8.69	0.36
8/3/18	11:00	M4	22.9	95	143	7.04	8.7	0.53	0.45	124	6.41	0.25
8/3/18	11:15	M5c	25.9	96	143	7.31	6.9	0.62	0.55	132	5.08	1.47
8/3/18	13:30	P1b	22.6	101	208	6.83	112.7	1.30	1.08	145	54.28	0.06
8/3/18	13:06	M6	26.6	111	165	7.71	10.8	0.53	0.44	93	5.41	0.65
8/22/18	17:27	K1	22.8	91	350	7.76	4.9	2.03	1.87	199	2.29	0.24
8/22/18	18:10	K2	25.6	76	387	8.27	13.8	4.89	4.05	227	6.71	0.55
8/22/18	17:00	M3	24.8	99	162	7.78	4.3	0.33	0.28	196	2.22	0.18
8/22/18	18:58	P2	25.2	75	227	8.58	18.5	0.48	0.31	188	12.75	1.51
8/22/18	18:35	M6	25.4	84	270	7.82	5.7	0.52	0.45	179	3.80	0.66
9/15/18	12:24	K1	22.0	95	282	7.56	6.5	1.57	1.28	141	2.58	0.06
9/15/18	12:55	K2	24.1	96	321	8.26	7.5	2.06	1.92	204	4.64	0.10
9/15/18	9:48	M1a	22.0	96	106	6.95	4.7	0.21	0.15	82	1.49	0.04
9/15/18	9:09	M2a	22.3	93	140	7.04	7.6	0.27	0.24	137	5.00	0.50
9/15/18	9:23	M1b	21.7	97	123	6.96	6.3	0.40	0.27	126	3.44	0.04
9/15/18	8:36	M3	23.0	96	159	7.28	11.7	0.50	0.37	145	7.95	0.18
9/15/18	10:38	M4	23.2	88	169	7.37	12.6	0.56	0.38	138	7.28	0.02
9/15/18	11:01	M5c	24.3	93	174	7.38	12.9	0.62	0.46	189	5.23	0.25
9/15/18	14:36	WOU	22.6	96	90	6.87	6.2	0.20	0.10	49	0.43	0.03
9/15/18	13:41	P1b	22.7	91	194	6.65	32.3	0.76	0.38	48	20.06	0.02
9/15/18	14:02	P2	29.7	105	237	9.23	15.5	0.49	0.28	158	9.70	0.27
9/15/18	13:20	M6	25.7	95	198	8.02	12.8	0.57	0.42	207	4.79	0.13
10/13/18	10:41	K1	21.6	97	325	7.71	8.5	2.68	2.60	253	5.04	0.18
10/13/18	11:05	K2	23.7	94	327	8.17	10.5	3.25	3.21	324	3.42	0.36
10/13/18	9:11	M1a	22.2	90	119	6.74	2.8	0.21	0.08	56	0.81	0.07
10/13/18	8:40	M2a	22.2	91	135	6.89	6.6	0.28	0.19	125	2.87	0.24
10/13/18	8:48	M1b	21.4	95	128	6.95	4.9	0.41	0.32	148	2.83	0.07
10/13/18	8:20	M3	22.6	99	154	7.44	9.1	0.37	0.30	168	5.16	0.16
10/13/18	9:47	M4	22.7	96	169	7.26	9.7	0.42	0.31	140	7.01	0.06
10/13/18	10:02	M5c	24.5	84	128	7.39	12.1	0.95	0.73	141	5.63	0.99
10/13/18	12:10	WOU	22.1	96	91	6.69	9.6	0.21	0.11	47	1.08	0.13
10/13/18	12:30	P1b	22.7	94	183	6.53	52.5	0.93	0.82	156	27.78	0.07
10/13/18	12:50	P2	31.1	110	211	9.51	23.0	0.64	0.47	177	3.91	1.23
10/13/18	11:22	M6	24.2	94	188	7.48	14.7	0.59	0.46	177	6.28	0.71
11/24/18	10:37	K1	20.7	95	320	7.74	9.2	2.62	2.04	341	7.11	0.22
11/24/18	11:02	K2	22.1	96	341	8.05	12.0	3.36	2.08	356	7.52	0.33
11/24/18	9:02	M1a	21.6	97	119	6.74	6.3	0.29	0.10	122	0.42	0.02
11/24/18	8:31	M2a	21.8	92	140	7.00	5.7	0.19	0.19	183	3.50	0.38
11/24/18	8:43	M1b	21.1	95	132	7.11	6.4	0.55	0.52	191	5.32	0.02
11/24/18	8:18	M3	21.8	95	162	7.53	7.8	0.25	0.21	146	5.22	0.02
11/24/18	9:44	M4	22.0	96	176	7.29	9.2	0.33	0.30	252	8.87	0.10
11/24/18	12:00	P1b	22.3	94	211	6.53	71.4	1.75	1.35	320	43.15	0.02
11/24/18	11:47	WOCM	22.3	95	130	6.91	12.0	0.28	0.25	233	8.72	0.12

Table 4. (Continued) Sample data. Time is Hawaiian Standard Time; Temp: temperature (°C); DO: dissolved oxygen (%); Cond: conductivity ($\mu\text{S cm}^{-1}$); TN: total nitrogen (μM); TP: total phosphorus (μM); PO4: orthophosphate (μM); SiOx: dissolved silicate (μM); N+N: nitrate and nitrite (μM); NH4: ammonium (μM).

Date	Time	Site	Temp	DO	Cond	pH	TN	TP	PO4	SiOx	N+N	NH4
11/24/18	12:22	P2	27.5	125	253	9.57	44.1	1.10	0.43	223	22.72	0.71
11/24/18	11:22	M6	23.0	92	208	7.46	23.2	0.53	0.37	272	12.15	0.40
12/15/18	8:37	K1	19.8	92	313	7.79	24.4	4.31	1.76	596	6.57	0.25
12/15/18	8:08	K2	20.3	94	342	7.65	14.2	3.73	1.39	643	2.98	0.11
12/15/18	9:20	M1a	20.5	96	119	6.82	7.9	0.23	0.05	56	0.54	0.12
12/15/18	9:42	M2a	20.7	93	132	7.01	13.9	0.25	0.16	134	3.73	0.60
12/15/18	10:01	M1b	20.4	97	132	7.27	9.0	0.81	0.23	113	2.26	0.08
12/15/18	10:23	M3	21.4	101	145	7.70	15.1	0.38	0.27	427	5.26	0.20
12/15/18	10:52	M4	21.0	93	183	7.37	30.9	0.65	0.23	460	5.59	0.04
12/15/18	11:04	M5c	21.6	91	187	7.50	21.5	0.94	0.26	436	6.69	0.26
12/15/18	12:05	WOU	20.9	97	135	6.67	7.3	0.29	0.13	67	0.78	0.09
12/15/18	12:22	P1b	21.7	92	221	6.52	55.4	2.30	0.33	120	13.01	0.05
12/15/18	12:42	P2	26.6	117	271	9.59	49.1	1.20	0.51	476	4.75	0.92
12/15/18	13:08	M6	22.5	98	217	7.58	26.0	0.63	0.49	484	10.95	0.69
1/26/19	11:35	K1	18.3	90	307	7.69	28.4	2.95	2.27	618	6.48	0.74
1/26/19	12:20	K2	19.7	91	319	8.14	8.0	4.12	2.71	545	2.14	0.39
1/26/19	9:45	M1a	18.6	89	116	6.79	8.6	0.27	0.12	199	1.05	0.27
1/26/19	8:52	M2a	18.5	91	107	6.80	21.5	0.32	0.17	194	3.46	2.98
1/26/19	9:10	M1b	19.0	94	124	7.39	8.6	0.68	0.35	267	4.00	0.15
1/26/19	8:25	M3	18.5	95	127	6.71	12.3	0.63	0.31	274	6.45	0.13
1/26/19	10:33	M4	18.7	89	136	7.11	15.3	0.53	0.34	389	10.28	0.15
1/26/19	10:46	M5c	20.2	86	144	7.39	15.9	1.38	0.80	286	5.98	1.39
1/26/19	13:13	WOU	19.0	93	94	6.73	15.3	0.31	0.12	116	4.20	0.19
1/26/19	13:36	P1b	21.5	85	205	6.73	163.5	3.36	2.67	852	####	0.53
1/26/19	14:08	P2	25.6	115	197	9.60	29.4	0.60	0.49	348	11.45	1.08
1/26/19	12:48	M6	20.8	98	170	7.46	20.1	0.54	0.29	376	4.86	0.53
2/23/19	11:07	K1	18.9	98	311	7.63	14.9	2.85	1.47	165	5.32	0.19
2/23/19	11:41	K2	21.1	99	333	7.92	11.8	3.46	1.48	192	2.75	0.18
2/23/19	9:22	M1a	20.0	98	121	6.59	2.3	0.25	0.15	201	1.25	0.10
2/23/19	8:42	M2a	19.7	92	141	7.05	8.1	0.27	0.12	96	2.33	0.81
2/23/19	8:57	M1b	19.8	97	129	7.18	6.8	0.56	0.39	218	5.03	0.14
2/23/19	8:21	M3	20.1	95	164	7.37	13.3	0.25	0.22	121	9.16	0.13
2/23/19	10:02	M4	20.3	97	179	7.36	18.1	0.52	0.25	204	12.25	0.25
2/23/19	10:24	M5c	22.4	91	190	7.48	16.2	0.85	0.27	131	4.16	0.39
2/23/19	13:16	P1b	22.2	94	227	6.59	118.3	3.01	0.90	193	88.07	0.10
2/23/19	12:45	WOCM	21.4	96	158	6.80	25.6	0.32	0.17	155	10.05	0.22
2/23/19	13:49	P2	27.9	133	314	9.79	50.7	0.82	0.36	134	19.98	0.81
2/23/19	12:07	M6	22.5	103	228	7.78	25.3	0.52	0.31	213	13.72	0.39
3/23/19	10:54	K1	19.6	98	315	7.60	17.1	3.90	2.40	268	6.56	0.25
3/23/19	11:15	K2	21.7	107	344	8.27	14.1	3.61	1.56	200	3.09	0.21
3/23/19	9:30	M1a	20.0	92	127	6.58	4.1	0.11	0.07	76	1.32	0.18
3/23/19	8:51	M2a	20.1	93	144	6.77	11.4	0.21	0.15	135	3.19	1.49
3/23/19	9:10	M1b	20.0	99	134	7.11	5.3	0.45	0.27	145	3.67	0.13
3/23/19	8:32	M3	20.8	100	158	7.25	8.8	0.37	0.26	246	1.66	0.46
3/23/19	10:13	M4	20.9	98	176	7.58	15.0	0.32	0.20	133	12.25	0.16
3/23/19	10:20	M5c	22.3	100	182	7.77	10.9	0.86	0.50	241	3.45	0.35
3/23/19	12:11	P1b	22.1	93	225	6.48	129.9	2.41	1.38	362	98.84	0.18
3/23/19	12:00	WOCM	21.4	96	161	6.74	17.6	0.62	0.42	232	8.94	0.23
3/23/19	12:34	P2	28.4	121	309	9.67	72.0	2.55	0.58	287	22.35	3.03
3/23/19	11:32	M6	22.8	111	234	7.88	26.1	0.52	0.40	202	13.90	0.44

REFERENCES

- Brereton, R. 2017. Nitrogen dynamics and retention in the river network of a tropical forest, Luquillo Mountains, Puerto Rico. Doctoral dissertation. Univ. of New Hampshire, Durham, <https://scholars.unh.edu/dissertation/2309>. Accessed 10 March 2021.
- Bruland, G. L., and G. DeMent. 2009. Phosphorus sorption dynamics of Hawai'i's coastal wetlands. *Estuaries and Coasts* **32**: 844-854. doi:10.1007/s12237-009-9201-9
- Chadwick, O. A., L. A. Derry, P. M. Vitousek, B. J. Huebert, and L. O. Hedin. 1999. Changing sources of nutrients during four million years of ecosystem development. *Nature* **397**: 491-497. doi:10.1038/17276
- Chadwick, O. A., E. F. Kelly, S. C. Hotchkiss, and P. M. Vitousek. 2007. Precontact vegetation and soil nutrient status in the shadow of Kohala Volcano, Hawaii. *Geomorphology* **89**: 70-83. doi:10.1016/j.geomorph.2006.07.023
- Chambers, R. M., and W. E. Odum. 1990. Porewater oxidation, dissolved phosphate, and the iron curtain: iron-phosphorus relations in tidal freshwater marshes. *Biogeochemistry* **10**: 37-52, <https://www.jstor.org/stable/1468568>. Accessed 16 January 2021.
- Chan, G., and A. Feeser. 2006. Waikīkī: a history of forgetting and remembering. University of Hawai'i Press.
- Clague, D. A., F. A. Frey, M. O. Garcia, S. Huang, M. McWilliams, and M. H. Beeson. 2016. Compositional heterogeneity of the Surtogloaf melilite nephelinite flow, Honolulu Volcanics, Hawai'i. *Geochim. Cosmochim. Acta* **185**: 251-277. doi:10.1016/j.gca.2016.01.034
- Cummins, K. W. 1974. Structure and functions of stream ecosystems. *BioScience*, **24**: 63-641, <https://www.jstor.org/stable/1296676>. Accessed 14 February 2021.
- Dashiell, E. P. 1997. Ala Wai Canal Watershed water quality improvement project: management and implementation plan, vol. 1. City and County of Honolulu, State of Hawaii.
- De Carlo, E. H., V. L. Beltran, and M. S. Tomlinson. 2004. Composition of water and suspended sediment in streams of urbanized subtropical watershed in Hawai'i. *Applied Geochem.* **19**: 1011-1037. doi:10.1016/j.apgeochem.2004.01.004
- De Carlo, E. H., and S. S. Anthony. 2002. Spatial and temporal variability of trace element concentrations in an urban subtropical watershed, Honolulu, Hawai'i. *Appl. Geochem.* **17**: 465-492. doi:10.1016/S0883-2927(01)00114-7
- Deenik, J., and A. T. McClellan. 2007. Soils of Hawai'i. *Soil and Crop Mgmt.* SCM-20, <http://hdl.handle.net/10125/12463>. Accessed 2 April 2021.

- Ellis, M. M. 1937. Detection and measurement of stream pollution. *Bull. U.S. Bur. Fish.* **48**: 365-437.
- Gavenda R., C. Smith, and N. Vollrath. 1998. Soils, p. 92-96. In: S. P. Juvik and J. O. Juvik [eds], Atlas of Hawaii. University of Hawaii Press, Honolulu.
- Giambelluca, T. W., Q. Chen, A. G. Frazier, J. P. Price, Y. -L. Chen, P. -S. Chu, J. K. Eischeid, and D.M. Delaparte. 2013. Online rainfall atlas of Hawai'i. *Bull. Am. Meteorol. Soc.* **94**: 313-316. doi:10.1175/BAMS-D-11-00228.1
- Gonzalez, F. I., Jr. 1971. Descriptive Study of the physical oceanography of the Ala Wai Canal. Master thesis, Univ. of Hawai'i at Mānoa, Honolulu.
- Hoover, D. J. 2002. Fluvial nitrogen and phosphorus in Hawai'i: storm runoff, land use, and impacts on coastal waters. Doctoral dissertation, Univ. of Hawai'i at Mānoa, Honolulu.
- Hoover, D. J., and F. T. Mackenzie. 2009. Fluvial fluxes of water, suspended particulate matter, and nutrients and potential impacts on tropical coastal water biogeochemistry: Oahu, Hawai'i. *Aquat. Geochem.* **15**: 547-570. doi:10.1007/s10498-009-9067-2
- Kirs, M., V. Kisand, M. Wong, R. A. Caffaro-Filho, P. Moravick, V. J. Harwood, B. Yoneyama, and R. S. Fujioka. 2017. Multiple lines of evidence to identify sewage as the cause of water quality impairment in an urbanized tropical watershed. *Water Res.* **116**: 22-33. doi:10.1016/j.watres.2017.03.024
- Kraft, B., H. E. Tegetmeyer, R. Sharma, M. G. Klotz, T. G. Ferdelman, R. L. Hettich, J. S. Geelhoed, and M. Strous. 2014. Nitrogen cycling. The environmental controls that govern the end product of bacterial nitrate respiration. *Science* **345**: 676-679. doi:10.1126/science.1254070
- Kuypers, M. M. M., H. K. Marchant, and B. Kartal. 2018. The microbial nitrogen-cycling network. *Nat. Rev. Microbiol.* **16**: 263-276. doi:10.1038/nrmicro.2018.9
- Laws, E. A., and L. Roth. 2004. Impact of stream hardening on water quality and metabolic characteristics of Waimānalo and Kāne'ohe Streams, O'ahu, Hawaiian Islands. *Pacific Science* **58**: 261-280, <http://hdl.handle.net/10125/2725>. Accessed on 17 November 2020.
- Michaude, J., and T. Wiegner. 2011. Stream nutrient concentrations on the windward coast of Hawai'i Island and their relationship to watershed characteristics. *Pacific Science* **65**: 195-217, <http://hdl.handle.net/10125/23220>. Accessed on 20 March 2021.
- Mortimer, C. H. 1941. The exchange of dissolved substances between mud and water in lakes. *J. Ecol.* **29**: 280-329. doi:10.2307/2256395

- Murphy, S. F., R.F. Stallard, M. C. Larsen, and W. A. Gould. 2012. Physiography, geology, and land cover of four watersheds in eastern Puerto Rico: chapter A in water quality and landscape processes of four watersheds in eastern Puerto Rico. USGS Professional Paper 1789. doi:10.3133/pp1789A
- Parsons, C. T., F. Rezanezhad, D. W. O'Connell, and P. Van Cappellen. 2017. Sediment phosphorus speciation and mobility under dynamic redox conditions. *Biogeosciences* **14**: 3585-3602. doi:10.5194/bg-14-3585-2017
- Paul, M. J., and J. L. Meyer. 2001. Streams in the urban landscape. *Annu. Rev. Ecol. Syst.* **32**: 333-365. doi:10.1146/annurev.ecolsys.32.081501.114040
- Rankin, E., B. Miltner, C. Yoder, and D. Mishne. 1999. Association between nutrients, habitat, and the aquatic biota in Ohio rivers and streams. *Ohio EPA Technical Bulletin* MAS/1999-1-1. Ohio Environmental Protection Agency, Columbus.
- Schopka, H. H., and L. A. Derry. 2012. Chemical weathering fluxes from volcanic islands and the importance of groundwater: the Hawaiian example. *Earth and Planetary Sci. Letters.* **339-340**: 67-78. doi:10.1016/j.epsl.2021.05.028
- Timbol, A. S., and J. A. Maciolek. 1978. Stream channel modification in Hawai'i part A: statewide inventory of streams, habitat factors and associated biota. Columbia (MO): US Fish and Wildlife Service, National Stream Alteration Team. FWS/OBS-78/16.
- Tomlinson M. S., and E. H. De Carlo. 2003. The need for high resolution time series data to characterize Hawaiian streams. *J. Am. Water Resour. Assoc.* **39**: 113-123. doi:10.1111/j.1752-1688.2003.tb01565.x
- USACE. 2015. Final independent external peer review report, Ala Wai Canal project, O'ahu Hawai'i feasibility study with integrated environmental impact statement. <https://usace.contentdm.oclc.org/digital/collection/p16021coll7/id/4422/>. Accessed on 10 January 2021.
- Vannote, R. B., G. W. Minshall, K. W. Cummins, J. R. Sedell, and C. E. Cushing. 1980. The river continuum concept. *Can. J. Fish. Aquat. Sci.* **37**: 130-137. doi:10.1139/f80-017
- Vitousek, P. M., J. D. Aber, R. W. Howarth, G. E. Likens, P. A. Matson, D. W. Schindler, W. H. Schlesinger, and D. G. Tilman. 1997. Human alteration of the global nitrogen cycle: Sources and consequences. *Ecol. Appl.* **7**: 737-750. doi:10.1890/1051-0761(1997)007[0737:HAOTGN]2.0.CO;2
- Walsh, C. J., A. H. Roy, J. W. Feminella, P. D. Cottingham, P. M. Groffman, and R. P. Morgan. 2005. The urban stream syndrome: current knowledge and the search for a cure. *J. N. Am. Benthol. Soc.* **24**: 706-723. doi:10.1899/04-028.1

- Weigelhofer, G., T. Hein, and E. Bondar-Kunze. 2018. Phosphorus and nitrogen dynamics in riverine systems: human impacts and management options. In S. Schmutz and J. Sendzimir [Eds.], *Riverine ecosystem management*. Aquatic Ecology Series, vol 8. Springer, Cham. doi:10.1007/978-3-319-73250-3_10
- Whittier, R. B., and A. I. El-Kadi. 2009. Human and environmental risk ranking of onsite sewage disposal systems for O‘ahu. Honolulu, HI: Univ. of Hawai‘i, <http://hdl.handle.net/10125/50770>. Accessed on 12 April 2021.
- Wymore, A. S., B. M. Rodriguez-Cardona, A. Herreid, and W. H. McDowell. 2019. LINX I and II: lessons learned and emerging questions. *Front Environ. Sci.* 7:181. doi:10.3389/fenvs.2019.00181
- Group 70 International, INC. 2005. Harold L. Lyon Arboretum, university of Hawai‘i conservation district use application: final environmental assessment. http://oeqc2.doh.hawaii.gov/EA_EIS_Library/2005-07-08-OA-FEA-Harold-Lyon-Arboretum.pdf. Accessed on 12 January 2021.